scientific reports

Check for updates

OPEN

Occurrence of spurious geostrophic currents on the marine geoid without horizontal gravity component

Peter C. Chu

This report clarifies the misconception in oceanographic community about the marine geoid and gravity, demonstrates the importance of horizontal gravity component in oceanography, and shows the misinterpretation of satellite-derived dynamic ocean topography. The marine geoid defines the hydrostatic equilibrium shape that the sea level would take in the absence of tides, currents, and winds. Under such a condition, geostrophic currents should vanish on the marine geoid. However, the gravity takes a 3D vector ($g = g_\lambda \mathbf{i} + g_\varphi \mathbf{j} + g_z \mathbf{k}$, called the real gravity) in geodesy and a vertical vector ($-g_0\mathbf{k}$, $g_0 = 9.81$ m/s^2, called the uniform gravity) in oceanography. Here, (i, j, k) are the unit vectors in the longitudinal (λ), latitudinal (φ), and vertical (z) directions of the reference ellipsoid. Due to such mismatch, the pressure gradient force balanced by the real gravity g (zero resultant force) on the marine geoid is no longer balanced by the uniform gravity ($-g_0\mathbf{k}$) (nonzero resultant force) and in turn generates spurious geostrophic currents. The present practice of using satellite observed dynamic ocean topography to represent the absolute geostrophic currents at the ocean surface is incorrect. Besides, inclusion of the horizontal gravity component becomes urgent in oceanography.

The marine geoid is an equipotential surface to represent the mean sea level without the influence of tides, currents, and winds. Usually, we do not observe the marine geoid directly, but use an Earth gravity field model to calculate its height (N) above the reference ellipsoid[1] with (λ, φ, z) being the (longitude, latitude, height) and ($\mathbf{i}$, $\mathbf{j}$, $\mathbf{k}$) being the corresponding unit vectors with eastward positive for $\mathbf{i}$, northward positive for $\mathbf{j}$, and upward positive for $\mathbf{k}$. Various global gravity field models have been developed to describe the three-dimensional Earth's disturbing gravity potential[2]. With satellite measurements, such as Gravity field and steady-state Ocean Circulation Explorer (GOCE)[3], Gravity Recovery and Climate Experiment (GRACE)[4], and combined GOCE-GRACE[5], several datasets of marine geoid N have been established in geodetic community,

$$z = N(\lambda, \varphi), \tag{1}$$

In conjunction with the satellite altimetry measurements[6,7] for the sea surface height relative to the reference ellipsoid (S) (waves and tides filtered out), the dynamic ocean topography (DOT), $D = S - N$, is calculated[8]. The oceanographic community uses N as the reference sea level and the horizontal gradient of DOT as the surface absolute geostrophic currents (AGC). The geodetic community uses such calculated surface AGC to verify static gravity models. This practice was originated in oceanography on the basis of the four believes which have never been tested: (1) small fluctuation of N ($\pm$ 1–2 m for the world oceans), (2) coincidence of equipotential and isobaric surfaces[9] on N [i.e., zero resultant force of the pressure gradient force and the real gravity $\boldsymbol{g}(\lambda, \varphi, z)$] with no geostrophic currents on N, (3) direct geostrophic calculation from the DOT to obtain the AGC on N, and (4) the AGC on the ocean surface defined by the AGC on N.

However, the gravity has three different forms: (1) the real gravity $\boldsymbol{g}(\lambda, \varphi, z)$ represented by a 3D vector field, (2) the normal gravity represented by a vertical vector $[-g(\varphi)\mathbf{k}]$ with latitudinal variation of intensity, and (3) the uniform gravity ($-g_0\mathbf{k}$, $g_0 = 9.81$ m/s^2). The real gravity ($\mathbf{g}$) is decomposed into

$$\mathbf{g} = \mathbf{g}_h + g_z\mathbf{k},\ \mathbf{g}_h = g_\lambda \mathbf{i} + g_\varphi \mathbf{j} \tag{2}$$

Naval Ocean Analysis and Prediction Laboratory, Department of Oceanography, Naval Postgraduate School, Monterey, USA. email: pcchu@nps.edu

Journal : SREP 41598 | Article No : 83063 | Pages : 8 | MS Code : 83063 | Dispatch : 29-1-2021

where $\mathbf{g}_h$ is the horizontal gravity component; and ($g_z\mathbf{k}$) is the vertical gravity component. The normal gravity vector [$-g(\varphi)\mathbf{k}$] is associate with a mathematically modeled Earth, which is a rigid and geocentric ellipsoid with a minor axis coinciding with the mean rotation of the Earth. This ellipsoid has the same total mass and angular velocity as the Earth[10], and more specifically is called the normal Earth or spheroid (i.e., an ellipsoid of revolution). Analogously to the real gravity $\mathbf{g}$, the normal gravity vector [$-g(\varphi)\mathbf{k}$] is the sum of the gravitational and centrifugal accelerations exerted on the water particle by the normal Earth. Its intensity $g(\varphi)$ is called the normal gravity. Several equations are available to compute the normal gravity. Among them, the World Geodetic System 1984 uses the Somiglina Eq. (11),

$$g(\varphi) = g_e\left[\frac{1+\kappa\sin^2\varphi}{\sqrt{1-e^2\sin^2\varphi}}\right],\ e^2 = \frac{a^2-b^2}{a^2},\kappa = \frac{bg_p - ag_e}{ag_e} \tag{3}$$

where (a, b) are the equatorial and polar semi-axes; a is used for the Earth radius, $R = a = 6.3781364\times10^6$ m; $b = 6.3567523\times10^6$ m; e is the spheroid's eccentricity; $g_e = 9.780$ m/s^2, is the gravity at the equator; and $g_p = 9.832$ m/s^2 is the gravity at the poles.

The uniform gravity ($-g_0\mathbf{k}$) is commonly used in oceanography. Such high simplification of the gravity leads to several popular viewpoints in the oceanographic community about the marine geoid, gravity disturbance, and horizontal gravity component such as fluctuation of the marine geoid (N) caused by the Earth eccentricity and not by the gravity disturbance, small fluctuation of the marine geoid ($|N|<1$–2 m), and negligible horizontal gravity component ($\mathbf{g}_h$). Questions arise: are these viewpoints correct? Does dynamic characteristics (e.g., hydrostatic equilibrium on the marine geoid N) keep the same with gravity changing from [$\boldsymbol{g}(\lambda, \varphi, z)$] to [($-g_0\mathbf{k}$)]? Does horizontal gradient of DOT represent the surface AGC as the present practice in both geodetic and oceanographic communities? To answer these questions, the basic gravity theory and global dataset of N generated in the geodetic community are first used to show the misconceptions on the marine geoid and horizontal gravity component in the oceanographic community. Then, a simple dynamical analysis is conducted to identify the difference between using the normal/uniform gravity without the horizontal gravity component and the real gravity with the horizontal gravity component, i.e., occurrence of spurious geostrophic currents on the marine geoid with the normal/uniform gravity. The present practice of using the horizontal gradient of DOT to represent the ocean surface AGC is proved incorrect. Finally, the importance of the horizontal gravity component in oceanography is demonstrated.

Fluctuation of marine geoid due to the gravity disturbance (not the Earth rotation)

Let (P, Q) be the Newtonian gravitational potential of the (real Earth, normal Earth) and P_R ($=\Omega^2 r^2\cos^2\varphi/2$) be the potential of the Earth's rotation. Let $W = P + P_R$ be the gravity potential of the real Earth (associated with real gravity $\mathbf{g}$) and $E = Q + P_R$ be the gravity potential of the normal Earth [associated with the normal gravity $-g(\varphi)\mathbf{k}$]. The gravity disturbance is the difference between the real gravity $\boldsymbol{g}(\lambda, \varphi, z)$ and the normal gravity [$-g(\varphi)\mathbf{k}$] at the same point[12]. The potential of the gravity disturbance (called the disturbing gravity potential) is given by

$$T = W - E = P - Q \tag{4}$$

Consequently, the centrifugal effect disappears and the disturbing gravity potential (T) can be considered a harmonic function. With the disturbing gravity potential T, the real gravity $\mathbf{g}$ is represented by

$$\mathbf{g}_h = \nabla_h T,\ g_z = -g(\varphi) + \frac{\partial T}{\partial z} \tag{5}$$

where ∇_h is the horizontal vector differential operator. The geoid height relative to the normal Earth (i.e., reference spheroid) is given by Bruns' formula[13]

$$N(\lambda,\varphi) = \frac{T(\lambda,\varphi,0)}{g_0} \tag{6}$$

Equations (4)–(6) clearly show that the fluctuation of the marine geoid is independent of the Earth rotation and dependent of the disturbing gravity potential (T) only.

Significant fluctuation of the marine geoid

Before satellites into practice, the fluctuation of the marine geoid was generally considered small over the world oceans (± 1–2 m). After satellites coming into practice, global geoid (N) datasets were established using the gravity field models together with satellite observed gravity data. Here, a static global combined gravity field model EIGEN-6C4 up to degree and order 2190 (a geodetic community model) is used for illustration. It was produced jointly by GFZ Potsdam and GRGS Toulouse and is posted at the website (http://dataservices.gfz-potsdam.de/icgem/showshort.php?id=escidoc:1119897) for public use[2,14]. The author ran the model with 1° × 1° resolution for 17 s to get the global N and found that N is fluctuated from − 106.20 to 85.83 m with the mean value of 30.57 m (Fig. 1), which is about 50–100 times larger than originally believed ($|N|<1$–2 m) by the oceanographic community. For example, $N = -99.76$ m at (80 °W, 3 °N) in the Indian Ocean, and $N = 65.38$ m at (26 °W, 45 °N) in the North Atlantic Ocean.

Journal : SREP 41598 | Article No : 83063 | Pages : 8 | MS Code : 83063 | Dispatch : 29-1-2021

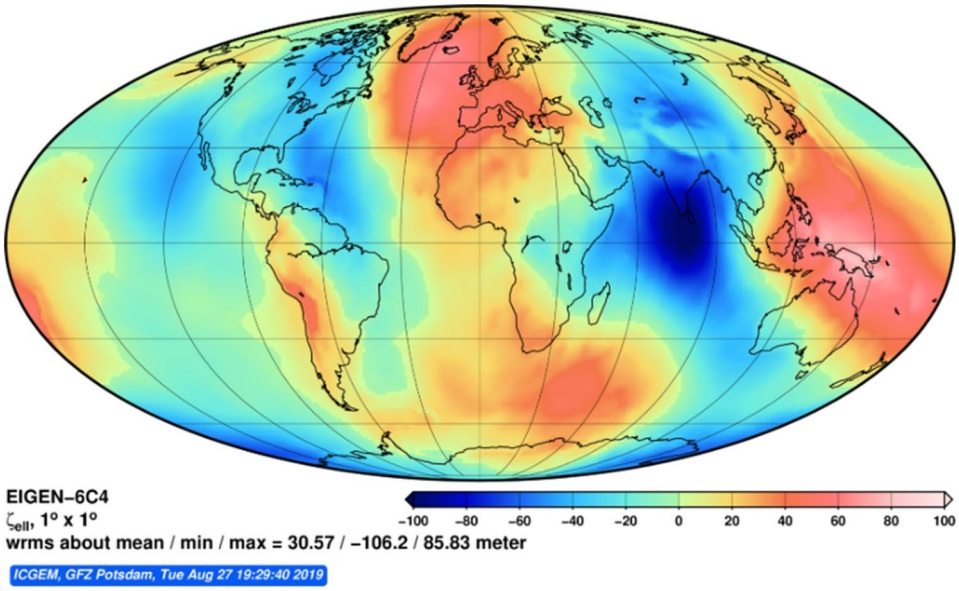

Figure 1. Digital data for EIGEN-6C4 geoid undulation (N) with 1°×1°, computed online at the website http://icgem.gfz-potsdam.de/home.

Non-negligible horizontal gravity component

Neglection of the horizontal gravity component $\mathbf{g}_h$ in oceanography has never been challenged since the normal gravity $g(\varphi)$ or uniform gravity g_0 is 5–6 orders of magnitudes larger than $|\mathbf{g}_h|$. However, vertical pressure gradient force is also 5–6 orders of magnitude larger than horizontal pressure gradient force in large-scale motion, but the horizontal pressure gradient force is never neglected against the vertical pressure gradient force.

Substitution of Eq. (6) into Eq. (5) leads to the connection of the horizontal gradient of the geoid N and the horizontal gravity components

$$\mathbf{g}_h = g_0 \nabla_h N \tag{7}$$

Since the fluctuation of marine geoid N is 50–100 times larger than the traditionally believed values (± 1–2 m), the importance of the horizontal gravity component ($\mathbf{g}_h$) in oceanography needs to be re-investigated. Generally, large-scale steady state oceanic motion with the horizontal gravity component is given by

$$\mathbf{k} \times (2\Omega \sin\varphi)\mathbf{u} = -\frac{1}{\rho}\nabla_h p + \mathbf{g}_h \tag{8}$$

where $\mathbf{u} = (u, v)$, is the geostrophic velocity vector; $\Omega = 2\pi/(86{,}400\ \text{s})$ is the Earth rotation rate. The horizontal vector differential operator ∇_h can be calculated using either the polar spherical coordinates or the oblate spherical coordinates (see "Appendix"). The difference between the two coordinates is less than 0.17%[15]. Here, the polar spherical coordinates are used for computational simplicity,

$$\mathbf{g}_h = g_0 \nabla_h N = g_0 \left[\mathbf{i} \frac{1}{R\cos\varphi} \frac{\partial N}{\partial \lambda} + \mathbf{j} \frac{1}{R} \frac{\partial N}{\partial \varphi} \right] \tag{9}$$

With the marine geoid height (N) data obtained from the EIGEN-6C4, the horizontal gravity components g_λ and g_φ are computed using Eq. (9). The histogram of the horizontal gravity intensity $|g_h|$ (Fig. 2) indicates a positively skewed distribution with a long tail extending to values larger than 12 mGal (1 mGal = 10^{-5} m/s^2). The statistical characteristics of $|g_h|$ are 2.084 mGal as the mean, 1.589 mGal as the standard deviation, 3.11 as the skewness, and 21.63 as the kurtosis.

The order of magnitude of $|\mathbf{g}_h|$ can be identified by a non-dimensional C-number from the scale analysis of $|\mathbf{g}_h|$ versus the Coriolis force in Eq. (8),

$$C = \frac{O(|\text{horizontal gravity}|)}{O(|\text{Coriolis force}|)} = \frac{g_0 O(|\nabla_h N|)}{fU} \tag{10}$$

where U is the scale of the horizontal velocity; and $f = 2\Omega\sin\varphi$, is the Coriolis parameter. With the mean value of $|g_h|$ (2.084 mGal) from the EIGEN-6C4 data, the corresponding geostrophic current speed is estimated by

Journal : SREP 41598 | Article No : 83063 | Pages : 8 | MS Code : 83063 | Dispatch : 29-1-2021

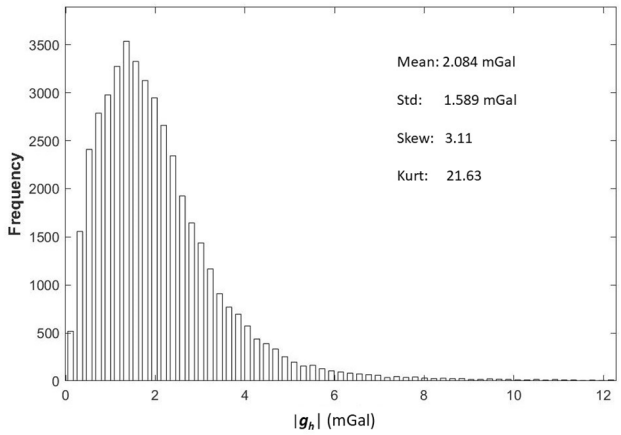

Figure 2. Histogram of the intensity of the horizontal gravity vector $|\mathbf{g}_h|$.

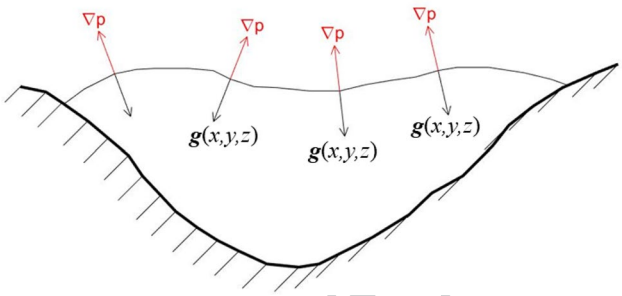

Figure 3. Three dimensional pressure gradient and real gravity $\boldsymbol{g}(x, y, z)$ on the geoid N.

$$U = g_0 O\left(\frac{|\nabla_h N|}{|f|}\right) = \frac{2.084\ \text{mGal}}{|f|},\ \text{for } C = 1 \tag{11}$$

Here, $U = 0.25$ m/s at 35° latitude. It demonstrates the importance of the horizontal gravity component ($\mathbf{g}_h$), which cannot be neglected.

Zero resultant force with the real gravity on the marine geoid

Generally, large-scale steady state ocean is in geostrophic motion,

$$\mathbf{k} \times (2\Omega \sin\varphi)\mathbf{u}_R = -\frac{1}{\rho}\nabla p + \mathbf{g}(\lambda, \varphi, z) \tag{12}$$

where $\nabla \equiv \nabla_h + \mathbf{k}\partial/\partial z$, is the three-dimensional vector differential operator; $\mathbf{u}_R = (u, v)$, is the geostrophic velocity vector using the real gravity $\mathbf{g}(\lambda, \varphi, z)$. Since the geoid is the equipotential surface coinciding with the isobaric surface, the direction of $\mathbf{g}(\lambda, \varphi, z)$ (i.e., the plumb line) is perpendicular to the geoid surface with the normal unit vector $\mathbf{n}$ (upward positive),

$$\mathbf{n} = -\frac{\mathbf{g}(\lambda, \varphi, z)}{|\mathbf{g}(\lambda, \varphi, z)|} \tag{13}$$

which parallels the pressure gradient force and real gravity (Fig. 3),

$$\mathbf{n} \bullet \left(\frac{\nabla p}{\rho}\right) = 0,\ \mathbf{n} \bullet \mathbf{g}(\lambda, \varphi, z) = 0 \tag{14}$$

with the hydrostatic equilibrium on the geoid (i.e., zero resultant force)

$$\left[-\frac{1}{\rho}\nabla p + \mathbf{g}(\lambda, \varphi, z)\right]_{z=N} = 0 \tag{15}$$

Journal : SREP 41598 | Article No : 83063 | Pages : 8 | MS Code : 83063 | Dispatch : 29-1-2021

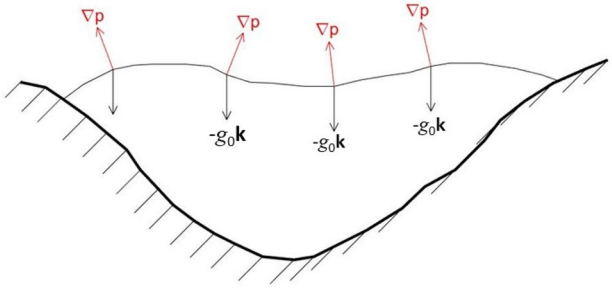

Figure 4. Three dimensional pressure gradient and uniform gravity ($-g_0\mathbf{k}$) on the geoid N.

Substitution of (15) into (12) leads to the vanish of geostrophic currents on N

$$\mathbf{u}_R|_{z=N} = 0, \text{ with the real gravity } \mathbf{g}(\lambda, \varphi, z) \tag{16}$$

Spurious geostrophic currents on the geoid with the normal/uniform gravity

When the real gravity $\mathbf{g}(\lambda, \varphi, z)$ is replaced by the normal gravity $[-g(\varphi)\mathbf{k}]$ or the uniform gravity $(-g_0\mathbf{k})$, the originally hydrostatic equilibrium by the 3D pressure gradient force $-(1/\rho)\nabla p$ and the 3D real gravity $\mathbf{g}(x, y, z)$ is destroyed due to the disappearance of the horizontal gravity component $\mathbf{g}_h$. Hereafter, the uniform gravity is taken for illustration. The nonzero resultant force of $-(1/\rho)\nabla p$ and $-g_0\mathbf{k}$ will generate spurious geostrophic currents on the geoid (Fig. 4),

$$\left[\mathbf{k} \times (2\Omega \sin\varphi)\mathbf{u}_N + \frac{1}{\rho}\nabla p + g_0\mathbf{k}\right]_N = 0 \tag{17}$$

Elimination of the pressure gradient force from Eqs. (15) and (17) and use of Eq. (2) lead to

$$\left[\mathbf{k} \times (2\Omega \sin\varphi)\mathbf{u}_N + \mathbf{g}_h + g_z\mathbf{k} + g_0\mathbf{k}\right]_N = 0 \tag{18}$$

Since the deviation of the vertical component of the gravity ($|g_z|$) to the uniform gravity (g_0) is about 3–4 orders of magnitude smaller than g_0, it is reasonable to assume

$$g_z \approx -g_0 \tag{19}$$

Thus, Eq. (18) becomes

$$[\mathbf{k} \times (2\Omega \sin\varphi)\mathbf{u}_N + \mathbf{g}_h]_N = 0 \tag{20}$$

which indicates that the missing horizontal gravity component $\mathbf{g}_h$ causes the occurrence of spurious geostrophic currents on the marine geoid. Substitution of Eq. (7) into Eq. (20) leads to

$$\mathbf{k} \times (2\Omega \sin\varphi)\mathbf{u}_N = -g_0\nabla_h N \tag{21}$$

With the global N data from the EIGEN-6C4, the spurious geostrophic currents due to the missing horizontal gravity component, $\mathbf{u}_N$, can be determined on the underwater marine geoid ($N \le 0$) using Eq. (21). The vector plot of $\mathbf{u}_N$ (Fig. 5a) and the color contour plot of the speed $|\mathbf{u}_N|$ (Fig. 5b) show evident oceanic motion on N due to the horizontal gravity component. Note that areas in the equatorial band (5 °S–5 °N) (geostrophic balance not valid) and with $N > 0$ are not included. The total number of grid points are 15,481. The histogram of $|\mathbf{u}_N|$ (Fig. 5c) indicates a positively skewed distribution with a long tail extending to values larger than 1.00 m/s. The statistical characteristics of $|\mathbf{u}_N|$ are 0.246 m/s as the mean, 0.208 m/s as the standard deviation, 1.567 as the skewness, and 4.909 as the kurtosis. The spurious geostrophic currents due to the missing horizontal gravity are evident and comparable to that due to the horizontal pressure gradient force[16–19].

Discussion

The hydrostatic equilibrium is the balance of gravity and pressure gradient force. Since the gravity has three forms (real, normal, and uniform), it is important to identify which one is used for the hydrostatic equilibrium on the marine geoid. Evidence presented here shows different outcomes on the same marine geoid: occurrence of spurious geostrophic currents using the normal gravity $[-g(\varphi)\mathbf{k}]$ or the uniform gravity $(-g_0\mathbf{k})$ and no motion using the real gravity $\mathbf{g}(\lambda, \varphi, z)$. The present practice using the horizontal gradient of DOT to represent the surface AGC[20–26] in both oceanographic and geodetic communities is incorrect due to (1) occurrence of spurious geostrophic currents with the mean value of 0.246 m/s on the marine geoid using the normal gravity $[-g(\varphi)\mathbf{k}]$ and the uniform gravity $(-g_0\mathbf{k})$, (2) significant fluctuation of marine geoid (− 106.20 to 85.83 m) from the community gravity model EIGEN-6C4, and (3) misrepresentation of the ocean surface AGC by the AGC on the marine geoid N. It is important to define the ocean surface on the reference ellipsoid (i.e., z = 0) and the surface

Journal : SREP 41598 | Article No : 83063 | Pages : 8 | MS Code : 83063 | Dispatch : 29-1-2021

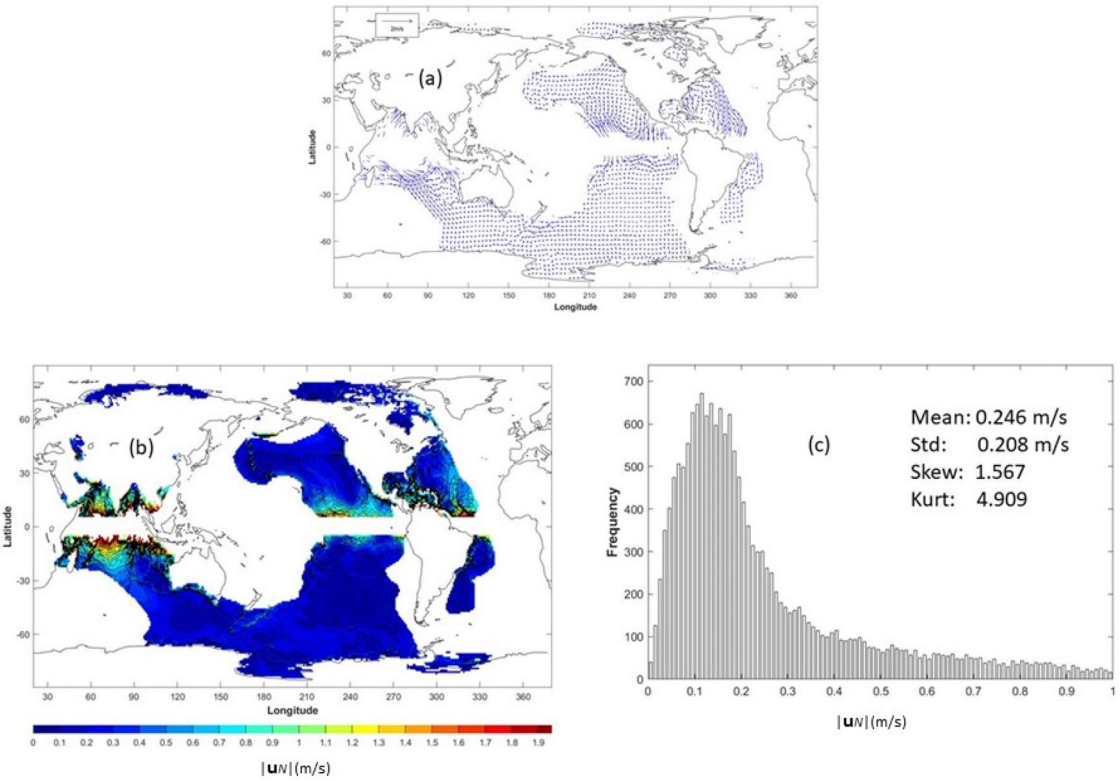

Figure 5. Spurious geostrophic currents due to the missing horizontal gravity component at underwater marine geoid: (**a**) vector plot of $\mathbf{u}_N$ (m/s), (**b**) contour plot of $|\mathbf{u}_N|$ (m/s), and (**c**) histogram of $|\mathbf{u}_N|$ (m/s). Note that areas in the equatorial (5 °S–5 °N) and with $N > 0$ are not included. The total number of grid points are 15,481. The source codes for the plots were written by the author's research group using the Matlab Version R2019b (https://www.mathworks.com/products/matlab.html).

AGC is the summation of the horizontal gradient of DOT, the AGC at the marine geoid, and the geostrophic shear due to inhomogeneous density[27,28].

Furthermore, a non-dimensional C-number is proposed to represent the relative intensity of the horizontal gravity component ($\mathbf{g}_h$) versus the Coriolis force. The horizontal gravity component ($\mathbf{g}_h$) has the similar intensity with the Coriolis force associated with the geostrophic current of 0.25 m/s at 35° latitude using the EIGEN-6C4 geoid data. Thus, inclusion of horizontal gravity component $\mathbf{g}_h$ becomes urgent in oceanography.

Appendix 1: Oblate spheroid coordinates versus polar spherical coordinates

This paper uses the polar spherical coordinates rather than the oblate spheroid coordinates for computational simplicity with a small error (0.17%). The oblate spheroid coordinates share the same longitude (λ) but different latitude (φ_{ob}) and radial coordinate (representing vertical) (r_{ob}). The relationship between the oblate spheroid coordinates (λ, φ_{ob}, r_{ob}) and the polar spherical coordinates (λ, φ, r) is given by[15]

$$r^2 = r_{ob}^2 + \frac{1}{2}d^2 - d^2 \sin^2 \varphi_{ob},\ r^2 \cos^2 \varphi = (r_{ob}^2 + \frac{1}{2}d^2) \cos^2 \varphi_{ob} \tag{22}$$

where d is the half distance between the two foci of the ellipsoid. For the normal Earth, $d = 521.854$ km. The vector differential operator in the oblate spheroid coordinates is represented by

$$\nabla = \mathbf{i}\frac{1}{h_\lambda^{ob}}\frac{\partial}{\partial \lambda} + \mathbf{j}\frac{1}{h_\varphi^{ob}}\frac{\partial}{\partial \varphi} + \mathbf{k}\frac{1}{h_r^{ob}}\frac{\partial}{\partial z},\ z = r - R \tag{23}$$

where $R = 6.3781364 \times 10^6$ m, is the semi-major axis of the normal Earth (Earth radius). The coefficients (h_λ^{ob}, h_φ^{ob}, h_r^{ob}) are given by

$$h_\lambda^{ob} = \sqrt{r^2 + \frac{1}{2}d^2}\cos\varphi,\ h_\varphi^{ob} = \sqrt{r^2 - \frac{1}{2}d^2 + d^2\sin^2\varphi},\ h_r^{ob} = \frac{r\sqrt{r^2 - \frac{1}{2}d^2 + d^2\sin^2\varphi}}{\sqrt{r^4 - \frac{1}{4}d^4}} \tag{24}$$

However, the vector differential operator in the polar spherical coordinates is represented by

Journal : SREP 41598 | Article No : 83063 | Pages : 8 | MS Code : 83063 | Dispatch : 29-1-2021

$$\nabla = \mathbf{i}\frac{1}{r\cos\varphi}\frac{\partial}{\partial\lambda} + \mathbf{j}\frac{1}{r}\frac{\partial}{\partial\varphi} + \mathbf{k}\frac{\partial}{\partial z} \tag{25}$$

Received: 29 July 2020; Accepted: 13 November 2020

References

1. Smith, W. H. F. The marine geoid and satellite altimetry. In *Oceanography from Space* (eds Barale, V. *et al.*) 217–232 (Springer, Dordrecht, 2010).
2. Ince, E. S. *et al.* ICGEM*15 years of successful collection and distribution of global gravitational models, associated services, and future plans. *Earth Syst. Sci. Data* **11**, 647–674 (2019).
3. Johannessen, J. A. *et al.* The European gravity field and steady-state ocean circulation explorer satellite mission its impact on geophysics. *Surv. Geophys.* **24**, 339–386 (2003).
4. Jet Propulsion Laboratory. *Gravity Recovery and Climate Experiment (GRACE)*. Science and mission requirements document, revision A, JPLD-15928, NASA's Earth Syst. Sci. Pathfinder Program, 1–84 (1998).
5. Bruinsma, *et al.* The new ESA satellite-only gravity field model via the direct approach. *Geophys. Res. Lett.* **40**, 3607–3612 (2013).
6. Fu, L. L. & Haines, B. J. The challenges in long-term altimetry calibration for addressing the problem of global sea level change. *Adv. Sp. Res.* **51**, 1284–1300 (2013).
7. Shum, C. K. *et al.* Calibration of JASON-1 altimeter over lake erie special issue: Jason-1 calibration/validation. *Mar. Geod.* **26**, 335–354 (2003).
8. Bingham, R. J., Haines, K. & Hughes, C. W. Calculating the ocean's mean dynamic topography from a mean sea surface and a geoid. *J. Atmos. Ocean. Technol.* **25**, 1808–1822 (2008).
9. Wunsch, C. & Gaposchkin, E.-M. On using satellite altimetry to determine the general circulation of the ocean with application to geoid improvement. *Rev. Geophys.* **18**, 725–745 (1980).
10. Vaníček, P. & Krakiwsky, E. *Geodesy: The Concepts* 697 (North-Holland, Amsterdam, 1986).
11. National Geospatial-Intelligence Agency. *Department of Defense World Geodetic System 1984 (WGS84)*. Its definition and relationships with local geodetic systems. NIMA TR8350.2, 3rd Edition, Equation 4–1 (1984).
12. Hackney, R. I. & Featherstone, W. E. Geodetic versus geophysical perspectives of the 'gravity anomaly'. *Geophys. J. Int.* **154**, 35–43 (2003).
13. Sandwell, D. T. & Smith, W. H. F. Marine gravity anomaly from Geosat and ERS 1 satellite altimetry. *J. Geophys. Res.* **102**(B5), 10039–10054 (1997).
14. Förste, C., Bruinsma, S.L., Abrikosov, O., Lemoine, J.M., Marty, J.C., Flechtner, F., Balmino, G., Barthelmes, F., & Biancale, R. EIGEN-6C4. The latest combined global gravity field model including GOCE data up to degree and order 2190 of GFZ Potsdam and GRGS Toulouse. https://doi.org/10.5880/icgem.2015.1 (2014).
15. Gill, A. E. *Atmosphere-Ocean Dynamics. International Geophysics Series, Vol 30* 91–94 (Academic Press, New York, 1982).
16. Yuan, D.-L., Zhang, Z.-C., Chu, P. C. & Dewar, W. K. Geostrophic circulation in the tropical north Pacific Ocean based on Argo profiles. *J. Phys. Oceanogr.* **44**, 558–574 (2014).
17. Chu, P. C. World ocean isopycnal level absolute geostrophic velocity (WOIL-V) inverted from GDEM with the P-Vector method. *Data* **3**, 1. https://doi.org/10.3390/data3010001 (2018).
18. Chu, P. C. & Fan, C. W. Absolute geostrophic velocity inverted from World Ocean Atlas 2013 (WOAV13) with the P-vector method. *Geosci. Data J.* **2**, 78–82. https://doi.org/10.1002/gdj3.31 (2015).
19. Chu, P. C. & Fan, C. W. Synoptic monthly gridded global and regional four dimensional WOD and GTSPP (T, S, u, v) fields with the optimal spectral decomposition (OSD) and P-vector methods. *Geosci. Data J.* **4**, 50–71. https://doi.org/10.1002/gdj3.48 (2017).
20. Tapley, B. D., Chambers, D. P., Bettadpur, S. & Ries, J. C. Large scale ocean circulation from the GRACE GGM01 geoid. *Geophys. Res. Lett.* **30**, 2163. https://doi.org/10.1029/2003GL018622 (2003).
21. Knudsen, P., Bingham, R., Andersen, O. & Rio, M.-H. A global mean dynamic topography and ocean circulation estimation using a preliminary GOCE gravity model. *J. Geod.* **85**, 861–879 (2011).
22. Sánchez-Reales, J. M., Vigo, M. I., Jin, S. & Chao, B. F. Global surface geostrophic ocean currents derived from satellite altimetry and GOCE geoid. *Mar. Geod.* **35**, 175–189 (2012).
23. Sudre, J., Maes, C. & Garçon, V. On the global estimates of geostrophic Ekman surface currents. *Limn. Oceanogr. Fluids Environ.* **3**, 1–20 (2013).
24. Jin, S., Feng, G. & Andersen, O. Errors of mean dynamic topography and geostrophic current estimates in China's marginal seas from GOCE and satellite altimetry. *J. Atmos. Ocean. Technol.* **31**, 2544–2555 (2014).
25. Rio, M.-H., Mulet, S. & Picot, N. Beyond GOCE for the ocean circulation estimate: Synergetic use of altimetry, gravimetry, and in situ data provides new insight into geostrophic and Ekman currents. *Geophys. Res. Lett.* **41**, 8918–8925 (2014).
26. Chang, C.-H., Kuo, C.-Y., Shum, C. K., Yi, Y. & Rateb, A. Global surface and subsurface geostrophic currents from multi-mission satellite altimetry and hydrographic data, 1996–2011. *J. Mar. Sci. Technol.* **24**, 1181–1193 (2016).
27. Chu, P. C. Two types of absolute dynamic ocean topography. *Ocean Sci.* **14**, 947–957 (2018).
28. Chu, P. C. A complete formula of ocean surface absolute geostrophic current. *Nat. Scie. Rep.* **Article number 10**, 1445 (2020).

Acknowledgements

The author would like to thank Dudley Chelton, Lee-Lueng Fu, Christopher W. Hughes, Armin Köhl, James C. McWilliams, Reiner Rummel, Frank Siegismund, Detlef Stammer, Andrew Stewart, and Carl Wunsch for invaluable discussion, Chenwu Fan for computational assistance, and the International Centre for Global Erath Models (ICGEM) for the EIGEN-6C4 geoid undulation data.

Author contributions

P.C.C. designed the project, conducted the analysis, and wrote the manuscript.

Competing interests

The author declares no competing interests.

Additional information

Correspondence and requests for materials should be addressed to P.C.C.

Journal : SREP 41598 | Article No : 83063 | Pages : 8 | MS Code : 83063 | Dispatch : 29-1-2021

Journal : **SREP 41598**	Article No : **83063**	Pages : **8**	MS Code : **83063**	Dispatch : **29-1-2021**